Estimation of the intracrystalline diffusion coefficient of the reactant during selective catalytic reduction of nitrogen oxide by propane on Co-ZSM-5

Takeshi Tabata * and Hirofumi Ohtsuka

Research and Development Department, Osaka Gas Co., Ltd., Torishima 6-19-9, Konohana-ku, Osaka 554, Japan
E-mail: ttabata@osakagas.co.jp

Received 6 May 1997; accepted 28 August 1997

In order to estimate the effect of diffusion during the selective catalytic reduction of nitrogen oxides (NOx) using propane on Co-ion-exchanged ZSM-5, the catalytic activity was measured for the catalysts prepared from zeolites having different crystal sizes. The conversions of NOx and propane on a catalyst having a large crystal size (1.3 μm) were much less than those on a catalyst having a smaller crystal size (0.10 μm). Based on the experimental data and certain assumptions, the effective intracrystalline diffusion coefficient of NO during the reaction in the presence of water vapor at 673 K was estimated to be $(6–9)\times10^{-15}$ m^2/s.

Keywords: intracrystalline diffusion, nitrogen oxide, propane, selective catalytic reduction, cobalt, ZSM-5

1. Introduction

Reducing nitrogen oxide (NOx) emissions from exhaust containing excess oxygen, such as the exhaust of diesel engines and lean-burn engines, is one of the most important problems to be solved for environmental protection. In 1990, it was reported that NOx is selectively reduced by hydrocarbons or alcohols even in the presence of excess oxygen on metal-ion-exchanged zeolite [1–5], H^+-form zeolite [6] and alumina [7].

It has been reported that selective catalytic reduction by hydrocarbons (HC-SCR) proceeds with high selectivity to NOx reduction (reduced NOx/consumed HC) on Co-based catalysts when light alkane is used as a reductant hydrocarbon [8–10]. Of the Co-based catalysts, a Co-zeolite catalyst is apparently superior to Co/Al_2O_3 for HC-SCR using propane [11], therefore, zeolite must play a certain role in this reaction. Since it has been reported that Co is well-dispersed without the formation of cobalt oxide agglomerates in Co-beta catalysts showing high selectivity [12], it is considered that zeolite at least contributes to the loading of Co with high dispersion. If the HC-SCR reaction occurred only on the surface of the zeolite crystal, the loading state of Co might be determined by defects on the crystal surface, and catalytic activity might not be related to the species or the micropore structure of zeolites. On the other hand, the HC-SCR activity of Co-zeolite catalysts seems to be strongly dependent on the species of zeolite [11], so that it is necessary to confirm whether the HC-SCR reaction proceeds in intracrystalline active sites or not in order to discuss the dependence on the zeolite structure.

Witzel et al. reported that the rate of N_2 formation in the HC-SCR using isobutane was clearly lower than that using methane on Co-ferrierite in the absence of water vapor, while these rates were comparable on Co-ZSM-5 [10]. This result strongly suggests that the HC-SCR reaction occurs in intracrystalline active sites since it is considered that isobutane cannot pass through the narrow cross connection made of an eight-membered ring in ferrierite causing the decrease in the diffusion rates of the reactants, while such inhibition of diffusion will not occur in ZSM-5, in which the channels are connected with ten-membered rings. However, it does not directly indicate that the HC-SCR reaction proceeds in intracrystalline active sites because it is also thought that the difference in the reaction mechanism between HC-SCR using methane and isobutane, which was not distinguished on Co-ZSM-5, happened to be enhanced on Co-ferrierite under the specific experimental conditions. Furthermore, whether intracrystalline active sites are used or not depends on the relative ratio between the reaction and diffusion rates which vary greatly according to reaction conditions.

Quite recently, Ogura et al. reported that SCR by methane occurred in the micropores of Ir/In/H-ZSM-5 because Ir, which acted as a promoter of NO oxidation into NO_2, was highly dispersed on the zeolite according to the hydrogen adsorption measurement [13]. However, a description of the number of the active sites which contribute to the reaction in the micropore is lacking.

In this paper, the effect of the diffusivity of the reactant of SCR using propane under actual HC-SCR conditions containing water vapor for the purification of the exhaust of a lean-burn gas engine is examined for Co-ZSM-5 catalysts having different crystal sizes, and it is

* To whom correspondence should be addressed.

attempted to estimate the intracrystalline diffusion coefficient of the reactant.

2. Theory

2.1. Assumptions

Since the reaction mechanism of HC-SCR has not been clarified, it is not possible to construct a strictly defined model. The following assumptions are used to analyze the effects of the diffusion:

(1) NO decreases only by one HC-SCR reaction, which is dependent on the concentrations of NO, C_3H_8 and O_2;

(2) C_3H_8 decreases by two reactions, one of which is the same HC-SCR reaction as in the assumption (1), the other is the simple oxidation reaction which is dependent on the concentrations of C_3H_8 and O_2.

Based on these assumptions, the mass balance equations including diffusion and reaction are expressed using a general phenomenological reaction rate form as follows:

$$\frac{\partial C_{NO}}{\partial t} = D_{NO}\Delta C_{NO} - k_v C_{NO}^n C_{C_3H_8}^m C_{O_2}^l , \tag{1}$$

$$\frac{\partial C_{C_3H_8}}{\partial t} = D_{C_3H_8}\Delta C_{C_3H_8} - Sk_v C_{NO}^n C_{C_3H_8}^m C_{O_2}^l - k_{vcomb} C_{C_3H_8}^{m'} C_{O_2}^{l'} , \tag{2}$$

$$\frac{\partial C_{O_2}}{\partial t} = \text{.....}$$

Here, C is the concentration of each species, assuming that the total pressure is atmospheric pressure; D is the diffusion coefficient of each species; k_v and k_{vcomb} are the reaction rate constants of HC-SCR and simple oxidation; S is the phenomenological ratio of the decrease of C_3H_8 / NO in the HC-SCR reaction.

Since the main products of the reactions, such as H_2O and CO_2, are the major components of the test gas, the concentrations of these species can be considered to be constant in the whole catalyst bed. The concentration of O_2 is also considered to be constant for the same reason. In contrast, NO and C_3H_8 are decreased by the reactions and their concentrations may be influenced by their diffusion. However, NO is so strongly adsorbed on Co [14,15], especially in the presence of oxygen [16], that its diffusion rate in the catalyst bed is considered to be quite lower than C_3H_8. Thus, the following third assumption is introduced:

(3) Only NO concentration spatially differs in the catalyst particles.

Thus, the eqs. (1) and (2) are transformed into

$$\begin{cases} \dfrac{\partial C_{NO}}{\partial t} = D_{NO}\Delta C_{NO} - k_{v0} C_{NO}^n C_{C_3H_8}^m & (3) \\ \dfrac{\partial C_{C_3H_8}}{\partial t} = -Sk_{v0} C_{NO}^n C_{C_3H_8}^m - k_{v0comb} C_{C_3H_8}^{m'} , & (4) \end{cases}$$

where the suffix v0 means the renormalized value involving the term of O_2 concentration as a constant value.

2.2. Reaction rate equations

At a stationary state, eq. (3) is equal to zero at each spatial position as follows:

$$\frac{\partial C}{\partial t} = D\Delta C - k_{v1} C^n \equiv 0 , \tag{5}$$

where D and C are the diffusion coefficient and concentration of NO, and k_{v1} is the renormalized rate constant involving the terms of O_2 and C_3H_8 concentrations as constant values.

On the other hand, the catalyst effectiveness factor can be expressed from the definition as

$$\eta \equiv \frac{k_{v1}^*}{k_{v1}} = \frac{\int C^n \, dv}{\int C_0^n \, dv} , \tag{6}$$

where k_{v1}^* is the observed rate constant calculated from the NO concentration at the surface of the catalyst (C_0).

Eqs. (5) and (6) are solved assuming spherical symmetry as described in the appendix. Although there may be an anisotropy in the intracrystalline diffusion, the assumption of spherical symmetry seems to be reasonable because ZSM-5 zeolite has a three-dimensional channel structure. Thus, eq. (6) is transformed into a well-known equation [17,18] using Thiele modulus φ:

$$\eta = \frac{3}{\varphi}\left(\frac{1}{\tanh\varphi} - \frac{1}{\varphi}\right) , \tag{7}$$

where

$$\varphi = r_0\sqrt{\frac{nk_{v1}C_0^{n-1}}{D}} , \tag{8}$$

and r_0 is the radius of the particle in which there is an NO concentration gradient.

Thus, using the NO concentration at the catalyst particle surface (C_{0NO}), eqs. (3) and (4) are finally transformed into

$$\begin{cases} \dfrac{dC_{0NO}}{dt} = -\eta k_v C_{0NO}^n C_{C_3H_8}^m C_{O_2}^l & (9) \\ \dfrac{dC_{C_3H_8}}{dt} = -\eta Sk_v C_{0NO}^n C_{C_3H_8}^m C_{O_2}^l - k_{vcomb} C_{C_3H_8}^{m'} C_{O_2}^{l'} , & (10) \end{cases}$$

where η is defined as eq. (7) and

$$\varphi = r_0\sqrt{\frac{nk_v C_{0NO}^{n-1} C_{C_3H_8}^{m} C_{O_2}^{l}}{D_{NO}}}. \qquad (11)$$

Since eqs. (9) and (10) express the reaction rates taking into consideration the effect of intraparticle diffusion at a certain position of the catalyst bed, the overall conversions of NO and C_3H_8 that are the only data experimentally obtained can be derived from the integration of these equations over the entire catalyst bed. Therefore, D_{NO} (and η) can be estimated from the experimental results using catalysts having different r_0.

2.3. Rate-determining step (intracrystalline diffusion vs. macropore diffusion)

It is usually considered that a catalyst pellet consists of primary particles of crystalline zeolite, and as a result, that the catalyst has macropores besides the intracrystalline micropores of the zeolite. Therefore, we must first consider whether the rate-limiting step is macropore diffusion or intracrystalline diffusion. If the macropore diffusion is the rate-determining step, r_0 and D_{NO} will be substituted by the radius of the catalyst pellet (R) and the diffusion coefficient in the macropore (D_{ma}); otherwise, these will be substituted by the radius of the primary crystalline zeolite (r) and the intracrystalline diffusion coefficient (D_{mi}), respectively. This can be seen from the following equations [19]:

$$\frac{D_{ma}}{R^2} \gg \frac{D_{mi}}{r^2}: \quad \text{rate-limiting stage} = \text{intracrystalline diffusion}, \qquad (12)$$

$$\frac{D_{ma}}{R^2} \ll \frac{D_{mi}}{r^2}: \quad \text{rate-limiting stage} = \text{macropore diffusion}. \qquad (13)$$

For the purpose of this paper, D_{ma} will estimated later assuming Knudsen diffusion or molecular diffusion to confirm that the condition of eq. (12) is fulfilled.

3. Experimental

3.1. Catalyst

Two kinds of NH_4-ZSM-5 ($SiO_2/Al_2O_3 = 50$) zeolites (N.E. Chemcat Co.), different in primary particle size, were used as a raw material for the experiments. ZSM-5(a) is a small crystalline zeolite and ZSM-5(b) is a large crystalline zeolite. Cobalt ion exchange was performed by suspending NH_4-ZSM-5 zeolites in an aqueous solution of cobalt acetate (0.006 M) at 333 K for 18 h. To adjust the ion exchange level, this ion exchange procedure was repeated six times for Co-ZSM-5(b), and twice for Co-ZSM-5(a). The ion-exchanged zeolites were washed, dried and pressed into tablets followed by crushing into particles of 1–2 mm, and then calcined in air at 773 K. For chemical and surface area analyses, ground samples were used.

3.2. Characterization of catalyst

The cobalt content was measured by ICP analysis and the ion exchange levels were calculated from the content of Co assuming that one Co ion (2+) is exchanged with two NH_4^+. The particle sizes of these catalysts were measured from an FE-SEM (Hitachi S-4000) image by averaging the diameter of a hundred primary particles based on the particle volume (the third power of the diameter). The pore distribution of these catalysts was measured by a porosimeter (Micromeritics Autopore II 9220). The surface area was measured by the BET one-point method (N_2) using an automatic BET surface area analyzer (Ohkura Riken). The measured BET surface area is not the outer surface of the zeolite crystal but the entire area including the inner surface of the micropores. The amount of CO adsorption was measured by the pulse method after heating at 773 K for 4 h in air as pretreatment using an automatic CO adsorption analyzer (Ohkura Riken). Raman spectra were measured as described elsewhere [12] using 514.5 nm radiation from an argon ion laser.

3.3. Catalytic activity test

Catalytic activity was measured in a fixed-bed flow reactor in a similar way to that described in the literature [20]. The test gas mixture (500 ppm NO, 1000 ppm C_3H_8, 1000 ppm CO, 660 ppm H_2, 10% O_2, 6% CO_2; dry gas base) was fed at a flow rate of 1 ℓ/min (GHSV = 15,000 h^{-1}) and water was added by a pump through a vaporizer to the gas mixture before entering the reactor. Gas was analyzed in the same ways as in the literature [20]. NOx and C_3H_8 conversions were defined as $2 \times$ (evolved N_2)/(inlet NO) and (inlet C_3H_8 − outlet C_3H_8)/(inlet C_3H_8), respectively.

4. Results

4.1. Results of the catalyst characterization

The SEM images of the catalysts are shown in figure 1. From analyses of these images, the diameters of the primary particles of Co-ZSM-5 were 0.10 μm for Co-ZSM-5(a) and 1.3 μm for Co-ZSM-5(b). As shown in figure 2, the catalysts have only one kind of macropore, with diameters of 0.06 μm for Co-ZSM-5(a) and 0.8 μm for Co-ZSM-5(b). Co ion exchange level, BET surface area, and the amount of CO adsorption are shown in table 1 with the above-mentioned data.

It is thought that Co ion exchange is not easy for Co-ZSM-5(b) because the diffusion of Co ions is quite slow

a

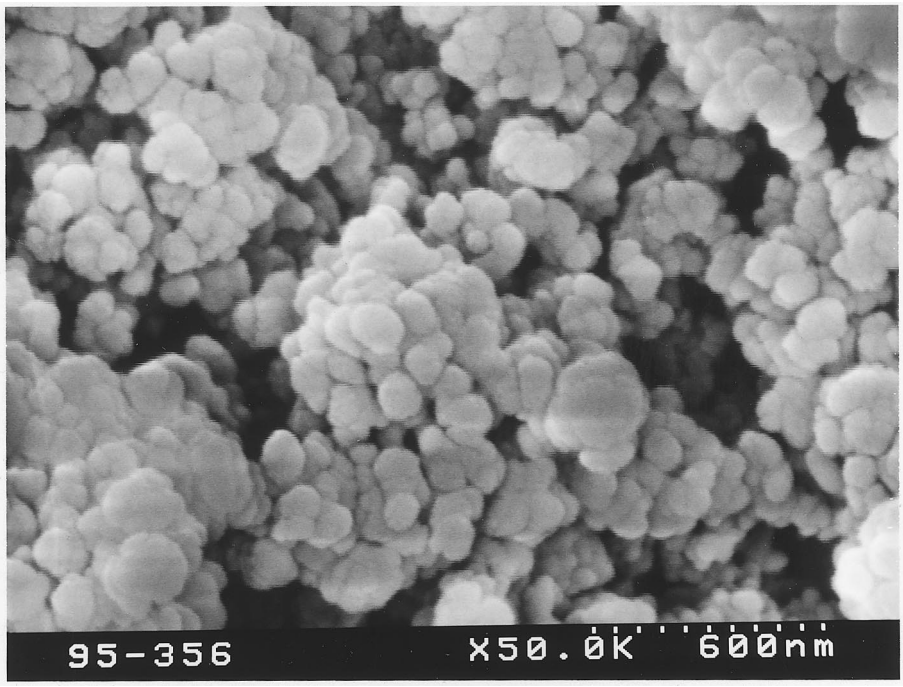

b

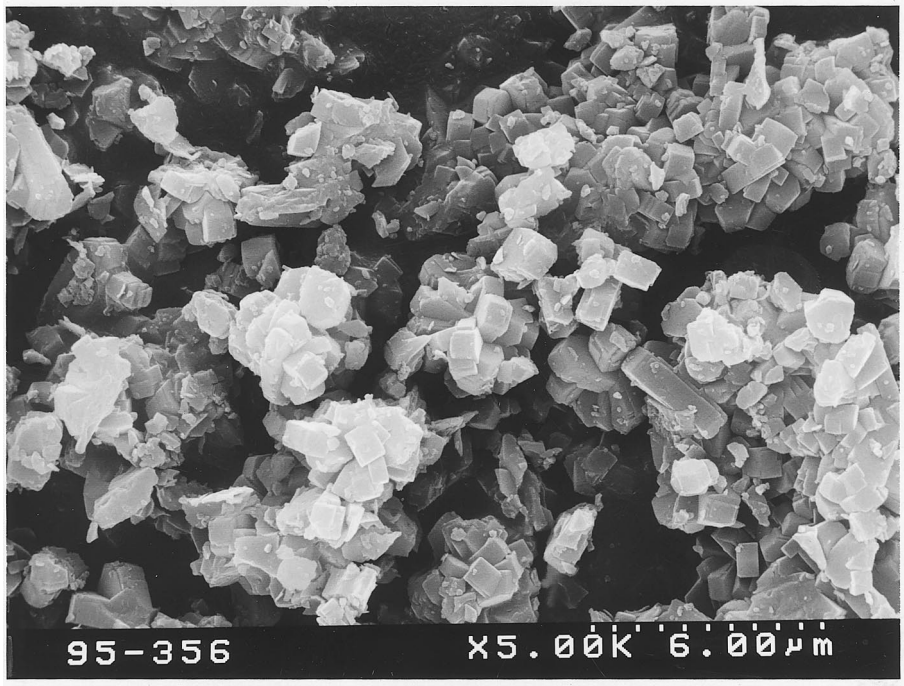

Figure 1. SEM images of Co-ZSM-5 catalysts. (a) Co-ZSM-5(a), ×50,000. (b) Co-ZSM-5(b), ×5,000.

in the large crystalline zeolite and Co may agglomerate on the crystal surface. If Co agglomerates and Co_3O_4 is formed, HC oxidation will be enhanced [12,21,22], and consequently, the analysis of the effects of the diffusion will be perturbed by the difference in the occurrence of Co_3O_4 between the two catalysts. When Co agglomeration occurs, even if very slightly, a Co_3O_4 signal can be observed with extremely high sensitivity in a Raman spectrum [12]. However, as shown in figure 3, almost no Co_3O_4 band at 690 cm^{-1} was observed in either the Co-ZSM-5(a) or (b) catalyst, while Co-ZSM-5 having 117% ion exchange level showed strong Co_3O_4 bands. Furthermore, there is no clear difference in the amount of CO adsorption between these two Co-ZSM-5 catalysts (table 1), and so, Co was dispersed well in the zeolite crystal in both catalysts.

4.2. Results of the catalytic activity test

The results of the HC-SCR activity tests of the Co-

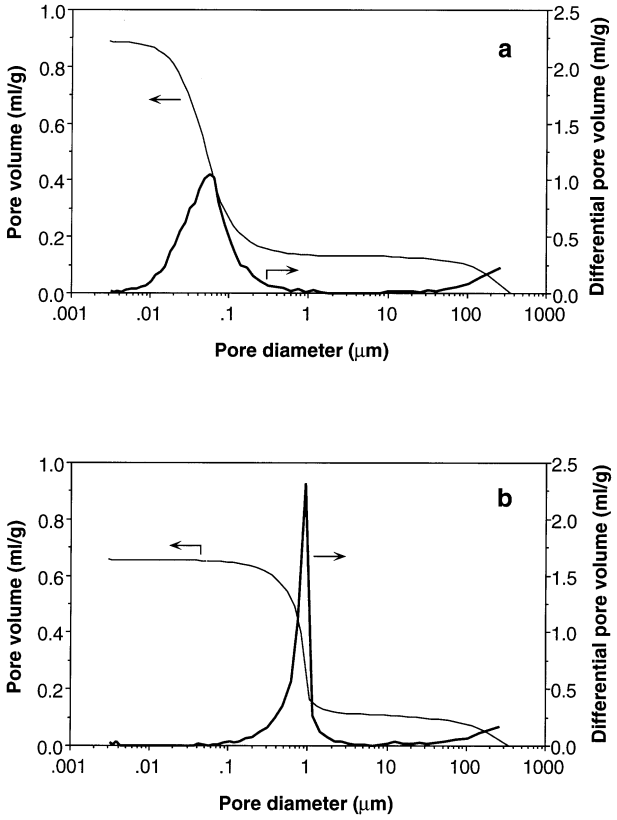

Figure 2. The pore distribution of Co-ZSM-5 catalysts. (a) Co-ZSM-5(a), (b) Co-ZSM-5(b).

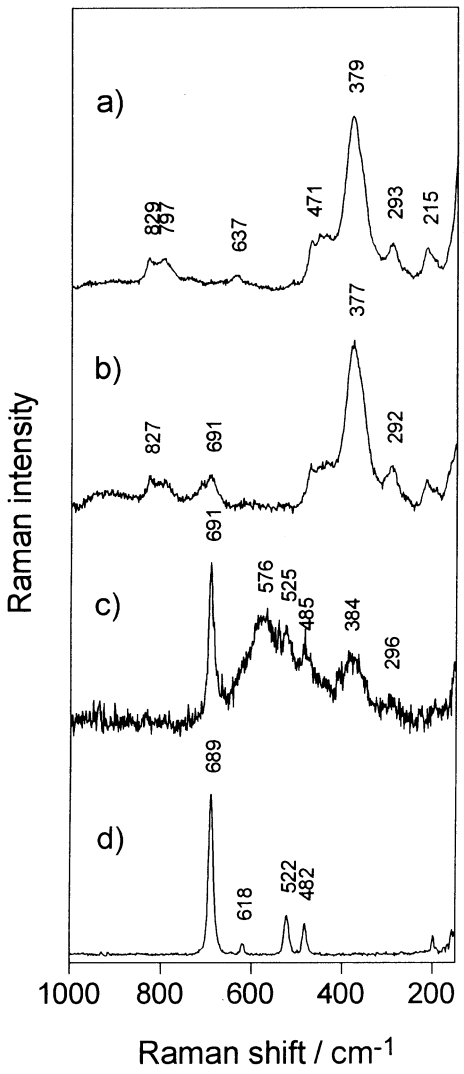

Figure 3. The Raman spectra of Co-ZSM-5 catalysts and a reference. (a) Co-ZSM-5(a), (b) Co-ZSM-5(b), (c) Co-ZSM-5 ($SiO_2/Al_2O_3 = 50$, ion exchange level = 117%), (d) Co_3O_4.

ZSM-5 catalysts are shown in table 2. Since the purpose is to evaluate the influence of diffusion on apparent HC-SCR activity under actual conditions, the test was carried out at 673 K. Both of the C_3H_8 and NOx conversions in table 2 are the steady state values and happen to be in a very appropriate conversion range for quantitative analysis. Table 2 shows that the apparent activity of Co-ZSM-5(b) is clearly lower than that of Co-ZSM-5(a).

4.3. Calculation of the reaction parameters and the catalyst effectiveness factors

Using the primary particle diameters in table 1, four parameters: k_v, D_{NO}, k_{vcomb}, and S are optimized by the numerical integration of eqs. (10) and (11) to fit the experimental overall conversions listed in table 2. The calculation was carried out by dividing the catalyst bed into 200 sections along the flow direction for two cases: $n = 1$ and $n = 2$. In both cases, $m = 1$ and $m' = 1$ are assumed for the reaction order of C_3H_8 concentration. The dependence on the O_2 concentration was also assumed to be of first order, but it affected only the dimension and the absolute value of k_v since C_{O_2} can be

Table 1
Results of the characterization of Co-ZSM-5 catalysts [a]

Item	Co-ZSM-5(a)	Co-ZSM-5(b)
primary particle diameter (μm)	0.10	1.3
macropore diameter (μm)	0.06	0.8
Co ion exchange level (%)	61	56
BET surface area ($m^2\,g^{-1}$)	341	288
CO adsorption (Nml g^{-1})	0.69	0.62

[a] $SiO_2/Al_2O_3 = 50$. Catalyst particle diameter = ca. 1.5 mm.

Table 2
Catalytic activity of Co-ZSM-5 catalysts for SCR using propane [a]

	Co-ZSM-5(a)	Co-ZSM-5(b)
NOx conversion (%)	47.1	14.4
C_3H_8 conversion (%)	54.7	29.7

[a] Reaction conditions: NO = 500 ppm, C_3H_8 = 1000 ppm, O_2 = 10%, H_2O = 9%, CO_2 = 6%, CO = 1000 ppm, H_2 = 660 ppm, He balance, GHSV = 15,000 h^{-1}, T = 673 K.

regarded as a constant value over the entire catalyst bed. In this calculation, the unit of concentration is represented in mol/m^3.

The results are listed in table 3. The catalyst effectiveness factor (η) differs along the catalyst bed since it explicitly contains $C_{C_3H_8}$. However, in both cases, the catalyst effectiveness factors of Co-ZSM-5(a) and Co-ZSM-5(b) are around 0.9 and below 0.2, respectively. Therefore, it may be concluded that the inner active sites were almost fully used on Co-ZSM-5(a) while only active sites quite near the surface of the crystal were used on Co-ZSM-5(b) under the experimental conditions. The calculated diffusion coefficient is dependent on the reaction order, but it can be estimated to be around $(6–9)\times10^{-15}\ m^2/s$ at 673 K.

5. Discussion

5.1. Confirmation of intracrystalline diffusion control

First of all, it must be confirmed that the influence of diffusion in the present experiment originates not in the macropore diffusion control but in the intracrystalline diffusion control. Both catalysts have only one kind of macropore, R and r in eq. (12) correspond to the radii of the catalyst pellet and of the primary particle of zeolite, respectively. In both catalysts, macropore diffusion is considered to be controlled by Knudsen diffusion since the macropore diameter is lower than 1000 nm [23]. The Knudsen diffusion coefficient D_k is represented by

$$D_k = \frac{2}{3} R \left(\frac{8 k_B T}{\pi m} \right)^{1/2}, \qquad (14)$$

Table 3
Results of the calculation of reaction parameters and catalyst effectiveness factors using the data in tables 1 and 2, and eqs. (7), (9)–(11)

Case 1 $n = 1, m = 1, m' = 1\ (l = 1, l' = 1)$		
parameters		
k_v $((m^3\ mol^{-1})^2\ s^{-1})$	2.13×10	
D_{NO} $(m^2\ s^{-1})$	6.31×10^{-15}	
k_{vcomb} $(m^3\ mol^{-1}\ s^{-1})$	0.190	
S	1.74	
catalyst effectiveness factor (η)	Co-ZSM-5(a)	Co-ZSM-5(b)
inlet of reactor	0.90	0.17
outlet of reactor	0.95	0.20
Case 2 $n = 2, m = 1, m' = 1\ (l = 1, l' = 1)$		
parameters		
k_v $((m^3\ mol^{-1})^3\ s^{-1})$	1.42×10^3	
D_{NO} $(m^2\ s^{-1})$	8.84×10^{-15}	
k_{vcomb} $(m^3\ mol^{-1}\ s^{-1})$	0.189	
S	1.76	
catalyst effectiveness factor (η)	Co-ZSM-5(a)	Co-ZSM-5(b)
inlet of reactor	0.82	0.12
outlet of reactor	0.95	0.15

where R, k_B, T, and m are pore radius, Boltzman constant, temperature, and mass of gas molecule, respectively [23]. Here, the diffusion coefficient of NO at 673 K in the macropore of Co-ZSM-5 catalysts can be calculated using eq. (14) and the D_k of Co-ZSM-5(a) and of Co-ZSM-5(b) are 1.4×10^{-5} and $1.8 \times 10^{-4}\ m^2/s$, respectively. These D_k and D_{NO} correspond to D_{ma} and D_{mi}, respectively, so that eq. (12) can be confirmed using the primary particle radius as follows, assuming that the radius of the catalyst sample particle is 0.75 mm and that the value $9 \times 10^{-15}\ m^2/s$ is adopted as D_{NO},

$$\frac{D_{ma}}{R^2} = 25 > \frac{D_{mi}}{r^2} = 3.6 \quad \text{(Co-ZSM-5(a))}, \qquad (15)$$

$$\frac{D_{ma}}{R^2} = 320 \gg \frac{D_{mi}}{r^2} = 0.021 \quad \text{(Co-ZSM-5(b))}. \qquad (16)$$

Thus, it can be concluded that the influence of the diffusion in the present experiment is controlled by intracrystalline diffusion, and so, D_{NO} can be identified as the intracrystalline diffusion coefficient under the present experimental conditions.

5.2. Adequacy of the assumptions

First, it should be confirmed that the reaction equations are reasonable from the aspects of the reaction mechanism. The reaction mechanism of HC-SCR using CH_4 on Co-zeolites has been relatively well examined. Li and Armor proposed a mechanism in which adsorbed NO_2 species, generated from adsorbed NO with oxygen, react with CH_4 to form $CH_3\cdot$ radicals on Co-ferrierite [16,24]. Cowan et. al reported, based on their isotopic exchange investigation, that the hydrogen abstraction from methane is considered to be the rate-determining step of HC-SCR using CH_4 on Co-ZSM-5 at around 673 K in the presence of water vapor and that adsorbed NO_2 may abstract the hydrogen [25]. Lukyanov et al. also reported that the reaction between NO_2 and CH_4 is the rate-determining step on Co-ZSM-5 below 500°C and that NO_2 formation is not the rate-determining step when O_2 is present in large amount [26]. On the other hand, Stakheev reported that NO_2 activates C_3H_8 to promote the HC-SCR reaction on Co-ZSM-5 with higher Co loading (above 60% ion exchange), although NO_2 formation is not a prerequisite for the reaction on Co-ZSM-5 with lower Co loading. From the literature, it can be assumed that the rate-determining step in the present case is the reaction between C_3H_8 and adsorbed NO_2 species, generated from NO and O_2, therefore, the assumption (1) is considered adequate.

Concerning the consumption of C_3H_8, it has been confirmed that the oxidation reaction without NO_x also proceeds to some extent under the present experimental conditions [11]. Further, Lukyanov et al. indicated that O_2 participates in the oxidation of an intermediate species of HC-SCR to reduce NO reduction selectivity

around 673 K [26]. Therefore, it would be appropriate to take into account the selectivity factor (S) in addition to the simple C_3H_8 oxidation by O_2. Thus, the assumption (2) as well as eq. (2) are considered adequate.

It is most important in the present analyses whether the diffusion of C_3H_8 is much faster than that of NOx. The intracrystalline diffusion rate is determined by the potential wall between molecule and pore. In the case of C_3H_8 on silicalite (ZSM-5), the activation energy of the intracrystalline diffusion is estimated by the NMR method to be around 7 kJ/mol [27], which is as little as the heat of physisorption. Co-ZSM-5 may adsorb C_3H_8 more strongly, but it has been reported that C_3H_8 is adsorbed on Co-ZSM-5 as strongly as NO or NO_2. In fact, we performed a TPD experiment and observed only one desorption peak of C_3H_8 below 333 K from Co-ZSM-5. Therefore, the adsorption of C_3H_8 on Co-ZSM-5 is considered to be as weak as physisorption and its heat is apparently considered to be much less than the heat of chemisorption of the NO_x which is not desorbed at 473 K [16]. Therefore, it seems reasonable to consider the assumption (3).

On the other hand, the question of whether NOx diffuses in the form of NO or NO_2 in the zeolite crystal should be also considered. It has been reported that the ratio of $NO_2/(NO + NO_2)$ is quite low in the gas at the outlet of the catalyst bed in the case of HC-SCR using C_3H_8 on Co-beta [12]. This means that NO_2 rapidly reacts with reductive compounds such as C_3H_8, CO and other intermediates into NO or N_2. Therefore, it is assumed here that NO_2 evolves only around active sites and does not diffuse so far without reacting into NO or N_2.

On the other hand, as for the accuracy of the calculated values, it should be noted that the values contain the errors derived from the distribution of crystal size in the catalyst, a difference in the crystal shape from a sphere, and a possible radial gradient of the concentration of the exchanged Co in the zeolite crystal.

5.3. Comparison with diffusion coefficient data in the literature

Although table 3 shows that the diffusion coefficient of NO is not strongly dependent on the reaction order of NO, it should be confirmed whether the reaction orders are appropriate. Li and Armor reported that the orders of NO and CH_4 are 0.7 and 0.8–0.9, respectively, in the case of $NO + CH_4 + O_2$ on Co-ferrierite in the presence of water vapor at 723–773 K. Therefore, the assumption of first order for both NO and C_3H_8 seems appropriate.

Zhang et al. measured the effective diffusion coefficients of NO on various metal-ion-exchanged ZSM-5 using a breakthrough curve during adsorption [28]. In the literature, the diffusion coefficient of NO in Co-ZSM-5 at 273 K was estimated to be 5.6×10^{-7} m^2/s, which is far larger than in the present analysis. However, the experiment reported in the literature was performed under the condition in which irrepressibly adsorbed species are saturated and ample gaseous NO exists in the pores. In such a case, a very rapid exchange occurs between the adsorbed molecules and the gaseous molecules, so called ''adsorption-assisted desorption'', which has been actually observed for this system [29]. In the case of adsorption-assisted desorption, desorption does not require the activation energy corresponding to adsorption heat, therefore, the diffusion of the adsorbate seems to proceed almost without potential wall. In fact, Zhang et al. indicated that the diffusion coefficient of NO is similar to that of Kr, which is not considered to be chemically adsorbed on zeolites. On the contrary, NO is diluted and decreased with the reaction in the present case, so that the adsorption-assisted desorption might not occur, and as a result, the diffusion of NO requires an activation energy corresponding to the adsorption heat of NO. Therefore, the extremely low effective diffusion coefficient of NO during the HC-SCR reaction is mainly due to the large adsorption heat of NO and additionally due to the inhibition by coexisting molecules such as H_2O and CO_2.

Finally, it may be worth mentioning when HC-SCR reaction is controlled by intracrystalline diffusion. Whether the diffusion controls the overall reaction rate can be judged from the catalyst effectiveness factor η, which can be calculated from eq. (7). For example, the values of η are 0.94, 0.80, 0.48, and 0.27 for $\varphi = 1$, 2, 5, and 10, respectively. Therefore, it can be concluded that the reaction rate is controlled by the diffusion under the conditions of $\varphi > 10$, while the influence of the diffusion can be neglected in the case of $\varphi < 1$. Here, Thiele modulus φ is the function of reactant concentrations, reaction rate constant of HC-SCR, diffusion coefficient, and primary particle size, as shown in eq. (11). It cannot be judged here whether published data are obtained under the conditions in which the diffusion did not control the reaction, because all data which appear in eq. (11) are not presented in literature, especially, primary particle size of zeolite. However, the primary particle diameter of commercially available ZSM-5 is usually around 0.1 μm, and so, we may extrapolate the present result for Co-ZSM-5(a) to published data for HC-SCR on Co-ZSM-5. If the experimental conditions including gas composition are similar to those in the present experiment, the influence of the diffusion may be neglected. It is considered that most published data for HC-SCR using methane on Co-ZSM-5 were not influenced by intracrystalline diffusion since the reaction rate of HC-SCR using methane on Co-ZSM-5 is considerably lower than that using propane. However, for HC-SCR using propane, when the product of the reactant concentrations in eq. (11) is 10 times larger than that in the present experiment, the effect of the diffusion cannot be neglected. The same conditions appear in the case of 10 times larger reaction rate constant or 10 times smaller

diffusion coefficient. However, these values are strongly influenced by the species and concentrations of co-existing molecules, such as water vapor or sulfur oxides, so that it is difficult to predict the influence of the diffusion in general.

6. Conclusion

The catalytic activity for HC-SCR using C_3H_8 on Co-ZSM-5 was measured in the presence of water vapor for the catalysts prepared from zeolites with different crystal sizes. The conversions of NOx and C_3H_8 on the catalyst with a large crystal size (1.3 μm) were much less than those on the catalyst with a smaller crystal size (0.10 μm). To estimate the diffusion coefficient of the reactant, the conversion results were analyzed under the following assumptions: (1) NO decreases by only one HC-SCR reaction which is dependent on the concentrations of NO, C_3H_8 and O_2; (2) C_3H_8 decreases by two reactions, one of which is the same HC-SCR reaction, the other of which is the simple oxidation reaction which is dependent on the concentrations of C_3H_8 and O_2; (3) only NO concentration spatially differs in the catalyst particles. The estimated value of the effective intracrystalline diffusion coefficient of NO during the reaction at 673 K was (6–9)$\times 10^{-15}$ m^2/s.

Acknowledgement

The authors wish to express their gratitude to N.E. Chemcat Corporation for providing the zeolite materials.

Appendix. Solution of the catalyst effectiveness factor for an *n*th order reaction

Assuming spherical symmetry, eq. (5) is expressed using polar coordinates by

$$\frac{D}{r^2}\frac{\partial}{\partial r}\left(r^2\frac{\partial C}{\partial r}\right) = k_{v1}C^n . \qquad \text{(A1)}$$

At $C \approx C_0$, the right side term can be expanded by C/C_0 and expressed by

$$\frac{D}{r^2}\frac{\partial}{\partial r}\left(r^2\frac{\partial C}{\partial r}\right) = k_{v1}C_0^n\left(n\frac{C}{C_0}+1-n\right). \qquad \text{(A2)}$$

This equation can be solved at $C \approx C_0$ and the result is

$$C = \frac{C_0}{n}\left(\frac{r_0}{\sinh(\alpha r_0)}\frac{\sinh(\alpha r)}{r}+n-1\right), \qquad \text{(A3)}$$

where

$$\alpha = \sqrt{\frac{nk_{v1}C_0^{n-1}}{D}}. \qquad \text{(A4)}$$

The differential of eq. (A3) at $C \approx C_0$ is expressed by

$$\frac{\partial C}{\partial r} = \frac{C_0}{n}\frac{r_0}{\sinh(\alpha r_0)}\left(\frac{\alpha r\cosh(\alpha r)-\sinh(\alpha r)}{r^2}\right), \qquad \text{(A5)}$$

and so, the differential towards the inside at the particle surface is

$$\left(\frac{\partial C}{\partial r}\right)_{r=r_0} = \frac{C_0}{n}\left(\frac{\alpha}{\tanh(\alpha r_0)}-\frac{1}{r_0}\right). \qquad \text{(A6)}$$

On the other hand, eq. (6) is transformed using eq. (A1) into

$$\eta = \frac{\int C^n \mathrm{d}v}{\int C_0^n \mathrm{d}v} = \frac{4\pi\int C^n r^2 \mathrm{d}r}{\frac{4}{3}\pi r_0^3 C_0^n} = \frac{3D}{r_0^3 C_0^n k_{v1}}\left[r^2\frac{\partial C}{\partial r}\right]_0^{r_0}. \qquad \text{(A7)}$$

Since there is no mass transfer at $r = 0$,

$$\left(\frac{\partial C}{\partial r}\right)_{r=0} = 0 . \qquad \text{(A8)}$$

Further, the value at $r = r_0$ is expressed by eq. (A6), and so, eq. (A7) is transformed into

$$\eta = \frac{3D}{r_0 C_0^n k_{v1}}\frac{C_0}{n}\left(\frac{\alpha}{\tanh(\alpha r_0)}-\frac{1}{r_0}\right)$$

$$= \frac{3}{\alpha r_0}\left(\frac{1}{\tanh(\alpha r_0)}-\frac{1}{\alpha r_0}\right), \qquad \text{(A9)}$$

and so, eq. (7) can be derived using the definition: $\varphi = \alpha r_0$.

References

[1] W. Held and A. König, German patent appl. DE 3642018 A1 (1987).
[2] Y. Fujitani, H. Muraki, S. Kondo and M. Fukui, Japanese patent appl. JP 63100919 A (1988).
[3] W. Held, A. König, T. Richter and L. Puppe, SAE Technical Paper Series No. 900496 (1990).
[4] M. Iwamoto, H. Yahiro, Y. Yu-u, S. Shundo and N. Mizuno, Shokubai (Catalysis) 32 (1990) 430.
[5] M. Iwamoto, H. Yahiro, S. Shundo, Y. Yu-u and N. Mizuno, Appl. Catal. 69 (1991) L15.
[6] H. Hamada, Y. Kintaichi, M. Sasaki, T. Ito and M. Tabata, Appl. Catal. 64 (1990) L1.
[7] Y. Kintaichi, H. Hamada, M. Tabata, M. Sasaki and T. Ito, Catal. Lett. 6 (1990) 239.
[8] H. Hamada, Y. Kintaichi, M. Sasaki, T. Ito and M. Tabata, Appl. Catal. 75 (1991) L1.
[9] Y. Li and J.N. Armor, Appl. Catal. B 1 (1992) L31.
[10] F. Witzel, G.A. Sill and W.K. Hall, J. Catal. 149 (1994) 229.
[11] T. Tabata, M. Kokitsu, H. Ohtsuka, O. Okada, L.M.F. Sabatino and G. Bellussi, Catal. Today 27 (1996) 91.
[12] H. Ohtsuka, T. Tabata, O. Okada, L.M.F. Sabatino and G. Bellussi, Catal. Lett. 44 (1997) 265.
[13] M. Ogura and E. Kikuchi, Chem. Lett. (1996) 1017.
[14] W.-X. Zhang, H. Yahiro, N. Mizuno, M. Iwamoto and J. Izumi, J. Chem. Soc. Faraday Trans. 91 (1995) 767.
[15] Y. Li and J.N. Armor, Appl. Catal. B 2 (1993) 239.
[16] Y. Li, T.L. Slager and J.N. Armor, J. Catal. 150 (1994) 388.
[17] E.W. Thiele, Ind. Eng. Chem. 31 (1939) 916.

[18] P.B. Weisz and C.D. Prater, Adv. Catal. 6 (1954) 143.
[19] D.M. Ruthven and K.F. Loughlin, Can. J. Chem. Eng. 50 (1972) 550.
[20] T. Tabata, M. Kokitsu and O. Okada, Appl. Catal. B 6 (1995) 225.
[21] M.C. Campa, S.D. Rossi, G. Ferraris and V. Indovina, Appl. Catal. B 8 (1996) 315.
[22] A.Yu. Stakheev, C.W. Lee, S.J. Park and P.J. Chong, Appl. Catal. B 9 (1996) 65.
[23] A. Wheeler, Adv. Catal. 3 (1951) 249.
[24] Y. Li and J.N. Armor, J. Catal. 150 (1994) 376.
[25] A.D. Cowan, R. Dumpelmann, and N.W. Cant, J. Catal. 151 (1995) 356.
[26] D.B. Lukyanov, E.A. Lombardo, G.A. Sill, J.L. d'Itri and W.K. Hall, J. Catal. 163 (1996) 447.
[27] L.V.C. Rees, Stud. Surf. Sci. Catal. 84 (1994) 1133.
[28] W.-X. Zhang, H. Yahiro, J. Izumi and M. Iwamoto, Nippon Kagaku Kaishi (J. Chem. Soc. Jpn.) (1994) 748.
[29] M. Iwamoto and Y. Hoshino, Chem. Lett. (1995) 729.